

Journal of Optoelectronical Nanostructures



Volume 11, Issue 1, Winter 2025, Page 1-101

Research Paper

Enhancing the Performance of Perovskite Solar Cells Using a Bilayer Electron Transport Layer Incorporating SWCNT

Mansureh Roohollahi¹, Mohammad Reza Shayesteh*,¹, Majid Pourahmadi¹

Received:

Revised:

Accepted: Published:

Use your device to scan and read the article online

Keywords:

SWCNT, Bilayer, Electron transport layer, Perovskite solar cell, chirality.

Abstract:

In this paper, a novel perovskite solar cell (PSC) structure incorporating a single-walled carbon nanotube (SWCNT) layer as a secondary electron transport layer (ETL) between the primary ETL and the top electrode is proposed and simulated. The electrical and optical effects of this additional layer on the PSC performance were investigated. Furthermore, the influence of nanotube chirality and the optimization of the SWCNT layer thickness were analyzed to enhance solar cell efficiency. Simulation results show that the incorporation of the SWCNT layer increases the conduction band slope in the perovskite layer, facilitating more efficient electron extraction and reducing recombination in this layer. Optically, the added layer reduces surface reflection and enhances light absorption within the perovskite layer thereby the short circuit current density (Jsc) is increased. As a result, the power conversion efficiency (PCE) of the proposed structure increased by 0.99% compared with the conventional PSC, reaching 20.39%.

Citation: Mansureh Roohollahi, Mohammad Reza Shayesteh, Majid Pourahmadi. Enhancing the Performance of Perovskite Solar Cells Using a Bilayer Electron Transport Layer Incorporating SWCNT.

Journal of Optoelectronical Nanostructures. 2025; 11 (1): 1-12

*Corresponding author: Mohammad Reza Shayesteh

Address: Department of Electrical Engineering, Yazd Branch, Islamic Azad University, Yazd, Iran. **Tell:** +98-3531871000 **Email:** shayesteh@iau.ir

¹ Department of Electrical Engineering, Ya.C., Islamic Azad University, Yazd, Iran.

1. INTRODUCTION

In today's world, the demand for energy in the industrial and residential sectors is very high. As non-renewable energy sources are being rapidly consumed, it is essential to utilize renewable energy sources as much as possible. Among the various renewable energy options, solar energy is a sustainable choice for global consumption planning [1]. Solar cells are promising devices that provide the possibility of meeting humanity's increasing energy needs by converting solar energy into electrical energy [2]. One of the materials that has recently entered this technology is perovskite. The beneficial optical and electronic properties that perovskite possesses, including high absorption coefficient, suitable carrier diffusion length, charge carrier mobility, and low production and manufacturing costs, have paved the way for the entry of perovskite solar cells (PSCs) as a promising technology for future generations of photovoltaics [3]. According to the "Best Research-Cell Efficiencies" chart published by the National Renewable Energy Laboratory (NREL), PSCs have achieved certified power conversion efficiencies exceeding 26% in recent years [4]. This remarkable progress has placed perovskites among the leading photovoltaic technologies, alongside crystalline silicon, CdTe, and CIGS, highlighting their strong potential for nextgeneration solar energy conversion.

In regular PSC structures, electron transport layers (ETLs) play an important role in the cell's efficiency because they prevent charge carrier recombination at the interface and improve cell performance. TiO₂ and SnO₂ are suitable options for ETLs because, in addition to having high mobility, they also have a suitable bandgap and provide good light transmission to the perovskite absorber layer [5, 6].

One novel approach to improve the performance of PSCs is to use a bilayer ETL instead of a single-layer structure. In such architectures, two different materials with complementary properties are sequentially positioned between the perovskite layer and the electrode[7]. The goal of this design is to simultaneously optimize several key factors, including increasing electron extraction, reducing carrier recombination, improving energy band alignment, and enhancing cell stability [8]. The use of dual ETLs results in a cascade-like conduction band alignment, which minimizes the energy mismatch between the perovskite layer and the electrode, leading to more efficient charge extraction and smoother electron flow [9]. Huang et al. discussed the use of Nb₂O₅/ZnO films as double ETLs in PSCs, enhancing power conversion efficiency and stability of the perovskite film through improved energy band matching and electron extraction

[10]. Lemos et al. explored the use of Nb₂O₅-Ti₃C₂ MXene/TiO₂ as an ETL in PSCs, highlighting its effective band alignment and stability, which enhance solar cell efficiency [11]. Sun et al. demonstrated that employing a bilayer ETL composed of TiO₂ and SnO₂ can significantly enhance the performance of PSCs. Their results showed an increase in power conversion efficiency by approximately 1.48% compared to mono-layer ETL device [8]. Table 1 presents some studies on bilayer ETL structures and their corresponding power conversion efficiencies in PSCs.

TABLE 1
Reported bilayer ETL structures and power conversion efficiency in PSCs

Device Structure	Efficiency	Reference
FTO/ZnO/Nb ₂ O ₅ / CH ₃ NH ₃ PbI ₃ / Spiro-OMeTAD/Ag	13.8	[10]
FTO/GQDs/TiO ₂ / CH ₃ NH ₃ PbI ₃ / Spiro-OMeTAD/Au	15.6	[12]
	17.64	[13]
ITO/TiO ₂ /SnO ₂ / CH ₃ NH ₃ PbI ₃ / Spiro-OMeTAD/Au	18.04	[14]
FTO/ TiO ₂ /ZnO/ FAPbI ₃ / Spiro-OMeTAD/Ag	18.24	[15]
$FTO/Nb_2O_5-Ti_3C_2/TiO_2/Cs0.17FA_{0.83}Pb(I_{0.83}Br_{0.17})_3/Spiro-OMeTAD/Au$	19.46	[11]

Among various nanomaterials investigated for improving the performance of PSCs, carbon nanotubes (CNTs) have attracted significant attention due to their exceptional electrical conductivity, excellent charge carrier mobility, and chemical stability [16, 17]. These unique properties make CNTs promising candidates for multiple roles in photovoltaic architectures, such as electrodes, charge transport layers, or even additive materials to improve interfacial contact and stability [18]. Several studies have demonstrated that incorporating CNTs into solar cell structures can enhance charge extraction, suppress recombination losses, and improve the efficiency [19, 20].

In this study, a novel PSC structure with bilayer ETLs is proposed. A single-walled carbon nanotube (SWCNT) layer is employed as the second ETL in the device structure. The energy level alignment between this layer and the primary ETL facilitates more efficient electron extraction. The simulation is performed

using the Silvaco TCAD software to analyze the optical and electrical behavior of the proposed structure. Simulation results indicate that the incorporation of the SWCNT layer contributes to the enhancement of the performance parameters of the PSC. In addition, the effect of nanotube thickness and chirality on the performance parameters of the solar cell was also investigated. Several experimental studies have demonstrated the effectiveness of incorporating carbon nanotubes into the ETLs of PSCs. For example, Arjmand et al. [21] reported a device employing a mesoporous TiO₂ ETL combined with MWCNT/Zn(COO)₂, which improved charge extraction and reduced interfacial recombination. In addition, Bati et al. [22] showed that the inclusion of SWCNTs into the ETL can effectively enhance the photovoltaic performance of PSCs. These findings suggest that the incorporation of CNTs into ETL design can yield promising results not only in theory but also in experimental studies, thereby providing a suitable basis for the development of novel architectures such as CNT-based bilayer ETLs.

To outline the overall structure of the paper, section 2 provides description of the theoretical modeling. Section 3 presents the structure of the proposed PSC with the incorporated SWCNT layer. Simulation results and performance analysis, including the investigation of electrical and optical effects, optimization of the carbon nanotube layer thickness, and the impact of nanotube chirality, are provided in Section 4 and finally, the conclusions are summarized in Section 5.

2. THEORETICAL MODELING

Years of research in semiconductor device physics have led to the development of a mathematical model that serves as a foundation for analyzing the electrical behavior of semiconductors. This model is applicable to various types of semiconductor devices such as solar cells. It consists of a set of fundamental equations that relate the electrostatic potential and the charge carrier densities within a defined simulation region. The electrical modeling is based on three main sets of equations. These equations include the Poisson equation, continuity equations, and drift-diffusion equations. Equation (1) represents the Poisson equation, which relates the electrostatic potential distribution to the total charge density [23].

$$\frac{\partial^2 \psi(x)}{\partial x^2} = \frac{q}{\varepsilon_0 \varepsilon_r} (n - p) \tag{1}$$

Where \mathcal{E}_0 and \mathcal{E}_r represent the vacuum permittivity and relative dielectric constant, respectively. P and n denote the hole and electron concentrations, while q is the elementary charge.

Equations (2) and (3) describe the continuity equations for electrons and holes, while Equations (4) and (5) correspond to the drift and diffusion equations respectively [23].

$$\frac{\partial n}{\partial t} = \frac{1}{q} \frac{\partial J_n}{\partial x} - R + G \tag{2}$$

$$\frac{\partial p}{\partial t} = -\frac{1}{q} \frac{\partial J_p}{\partial x} - R + G \tag{3}$$

Where R is recombination rate and G is generation rate.

$$J_n(x) = -qn(x)\mu_n \frac{\partial \psi(x)}{\partial x} + qD_n \frac{\partial n(x)}{\partial x}$$
(4)

$$J_p(x) = -qp(x)\mu_p \frac{\partial \psi(x)}{\partial x} - qD_p \frac{\partial p(x)}{\partial x}$$
 (5)

Where D_n and D_p are the diffusion coefficients of electrons and holes.

The above set of equations provides the necessary framework for simulating the electrical behavior of semiconductor devices, such as PSCs, and enables the analysis of the device's performance parameters.

3. PROPOSED PEROVSKITE SOLAR CELL AND SIMULATION PARAMETERS

The architecture of PSCs is relatively simple, typically consisting of a perovskite light-absorbing layer sandwiched between an ETL and a hole transport layer (HTL). Energy band alignment ensures that light-generated electrons are selectively transported towards the ETL, while hole transport in the same direction is energetically unfavorable. Conversely, the HTL facilitates the movement of holes towards the electrode and prevents electron passage. In common PSC structures, TiO₂ is usually used as the ETL and Spiro-OMeTAD as the HTL.

Fig. 1 shows a typical energy band diagram of a PSC. The conduction band offset (CBO), also indicated in the figure, refers to the energy difference between the conduction bands of the perovskite and ETL. A smaller CBO generally leads to better solar cell performance [23]. Additionally, the Φ value represents the energy difference between the conduction band of the ETL and the work function

of the cathode. An increase in Φ results in a decrease in device performance [23]. This performance loss is associated with the conduction band slope of the perovskite, as illustrated in Fig. 2. As Φ increases, the internal electric field across the perovskite layer weakens, the conduction band becomes flatter, and charge carrier recombination within the perovskite layer increases. Consequently, the overall efficiency of the solar cell declines with increasing Φ .

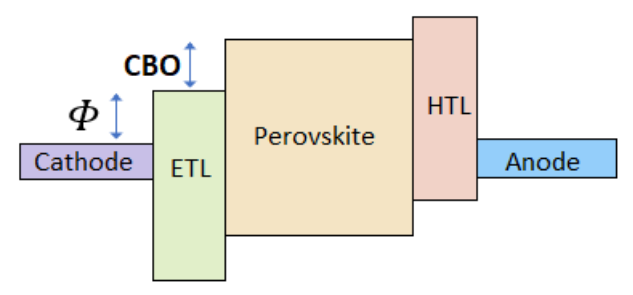


Fig. 1. Energy band diagram of a typical PSC

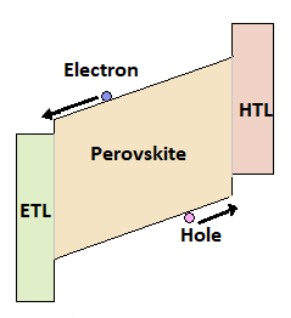


Fig. 2. Conduction band bending in the perovskite absorber layer

As explained earlier, improving the performance of PSCs requires minimizing both the CBO and the Φ value, but Fig. 1 shows that reducing CBO leads to increase in Φ . achieving an optimal balance between these two parameters is challenging, as changes in one affect the other. An effective strategy to reduce the Φ value while maintaining a desirable CBO level is the use of two ETLs, which leads to more efficient carrier extraction [23]. This structure is shown in Fig. 3.

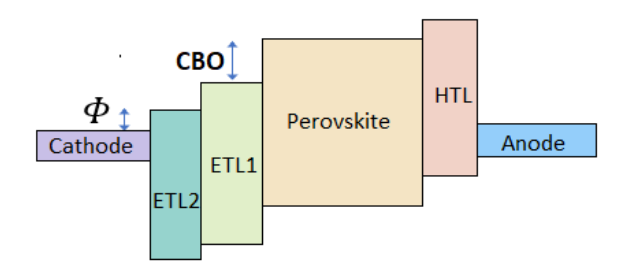


Fig. 3. The bilayer ETL structure and its effect on reducing the Φ value

Graphene consists of carbon atoms arranged in a honeycomb (hexagonal) lattice. When this two-dimensional sheet is rolled into a cylinder, a carbon nanotube is formed. Carbon nanotubes can be classified into two main types: single-walled and multi-walled nanotubes. Single-walled carbon nanotubes (SWCNTs) are composed of a single layer of graphene rolled into a cylindrical shape, whereas multi-walled carbon nanotubes (MWCNTs) consist of multiple concentric graphene layers rolled similarly.

To describe the geometric structure of a carbon nanotube, a vector called the chiral vector is defined. The chiral vector is determined by two integers, n and m, which represent the number of unit vectors along the two directions a_1 and a_2 in the hexagonal graphene lattice. This vector, defined by Equation (6), plays a key role in determining the electronic properties of the nanotube, such as whether it behaves as a metal or a semiconductor.

$$C_h = na_1 + ma_2 \tag{6}$$

SWCNTs and MWCNTs differ in diameter, and this difference significantly affects their electrical and mechanical properties. Equation (7) defines the relationship between the indices n and m and the diameter of the carbon nanotube [24].

$$D_{CNT} = \frac{a_0}{\pi} \sqrt{n^2 + m^2 + mn} \tag{7}$$

where a_0 is represents the carbon-carbon bond length in the graphene lattice. Additionally, Equation 8 describes the correlation between the nanotube diameter and its bandgap energy [25].

$$E_g = \frac{2a_0 Epi}{D_{cnt}} \tag{8}$$

where E_{pi} is carbon bond tight binding energy parameter.

To enhance the performance of the PSC, we propose a novel structure by incorporating a SWCNT layer as a secondary ETL. The proposed structure is shown in Fig. 4. TiO₂ is the first ETL and the perovskite used in this study is methylammonium lead iodide (CH₃NH₃PbI₃). Figure 4b shows the energy level diagram of this propose structure. Details of the physical parameters used in numerical simulation for the various layers in this structure are listed in Table 2 [26, 27]. In this work, the numerical simulations were carried out using a steadystate drift-diffusion model that does not explicitly account for mobile ionic species or slow-response traps. As a result, the model is inherently timeindependent and does not reproduce the scan-direction dependence (hysteresis) typically observed in experimental perovskite solar cells. It is well established in the literature that hysteresis mainly arises from ion migration and/or slow trapping phenomena, and a more explicit representation of this effect would require the inclusion of mobile ionic species or dynamic elements such as ionic capacitors or time-dependent trap-assisted recombination[28], which are beyond the scope of the present study. Nevertheless, it should be noted that in some experimental studies with similar structures incorporating SWCNT and TiO₂, a remarkable suppression of hysteresis has been reported [22, 29], which supports the plausibility of minimized hysteresis in the present architecture.

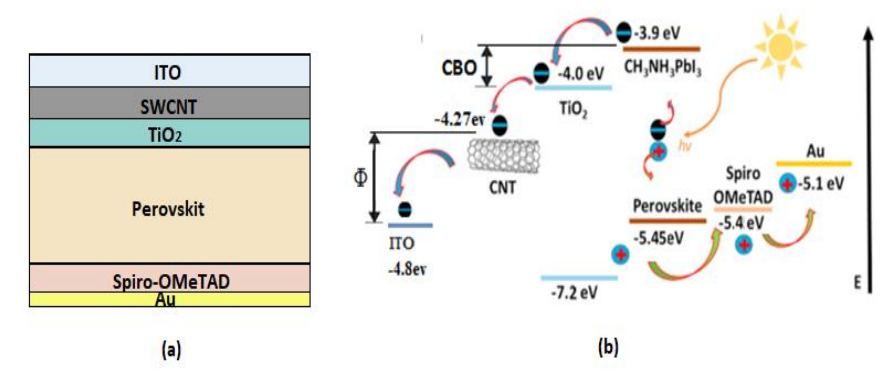


Fig. 4. (a) Proposed structure of the solar cell; (b) Corresponding energy level diagram

TABLE 2
Physical parameters of device layers used in numerical simulation

I hysical parameters of device layers used in numerical simulation						
Parameter	Layer	ETL1	ETL2	Absorber	HTL	
	Material	SWCNT	TiO ₂	CH ₃ NH ₃ PbI ₃	Spiro-	
					OMeTAD	
Thick	ness	0.2	0.1	0.5	0.2	
(µm	1)					
Dielectric pe	ermittivity	3.4	19	100	3	
Valance band						
effective de	ensity of	5e16	2e19	2e19	1.9e19	
state	es					
(cm	-3)					
Conduction	on band					
effective de	ensity of	6e17	2e18	2e18	2.2e18	
state	_					
(cm	-3)					
Hole mo	bility					
μ_p		2e3	0.1	1	2e-4	
(cm ² /v	.sec)					
Electron n	nobility					
μ_n		8e3	0.2	1	2e-4	
(cm ² /v	.sec)					

4. SIMULATION AND RESULTS

The aim of this study is to propose a bilayer ETL structure for PSCs, in which the second ETL is composed of SWCNT layer with a chirality of (6,5). To evaluate the effectiveness of this layer, both its electrical and optical effects are investigated. Moreover, the impact of the carbon nanotube chirality on the device performance is also presented. The simulation was carried out under AM1.5 illumination conditions.

1) Evaluation of the Electrical Effectiveness of SWCNT layer

This section investigates the electrical effects of the carbon nanotube layer and its contribution to enhanced electron transport and improved solar cell performance. As shown in Fig 4b, after the addition SWCNT layer, the value of Φ decreases from 0.8 to 0.53 eV. This reduction leads to an increase in the conduction band slope within the perovskite layer. A steeper conduction band facilitates electron transport. Consequently, as electrons are extracted more rapidly from the absorber layer, their recombination rate within the perovskite is reduced. As a result, more charge carriers reach the electrodes, leading to improved device performance. Figures 5 and 6 respectively present the simulation

results before and after incorporating carbon nanotubes, highlighting the changes in the conduction band slope and the carrier recombination rate within the perovskite layer.

As shown in Fig. 5, the addition of the SWCNT layer leads to an increase in the conduction band slope in the perovskite layer. In fact, the addition of this layer causes a change in the charge density in the cell layers, and according to Poisson's equation, any change in charge leads to a change in the electric field and a change in the slope of the energy bands.

Fig. 6 compares the carrier recombination rate in the perovskite layer. As observed, after adding the SWCNT layer, the recombination rate significantly decreased. The reason for this is that the improved conduction band slope accelerates electron transfer and reduces their presence time in the perovskite layer. In fact, SWCNT guides electrons faster towards the electrode, and their probability of recombination with holes in the perovskite becomes lower. This reduction in recombination directly leads to an increase in current density and an improvement in solar cell efficiency.

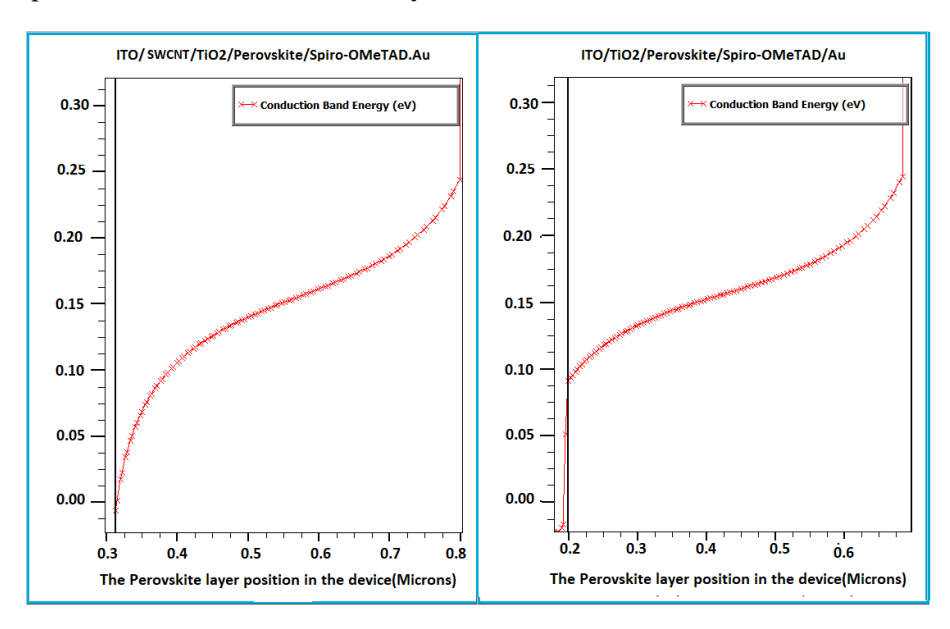


Fig. 5. Conduction band slope in the perovskite layer before and after incorporation of the SWCNT layer

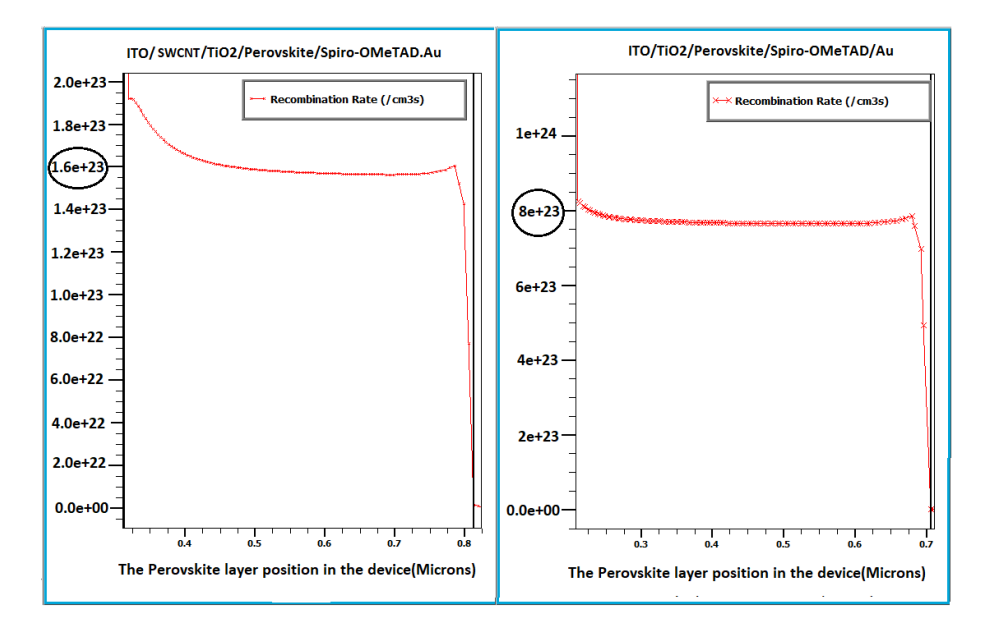


Fig. 6. Recombination rate in the perovskite layer before and after incorporation of the SWCNT layer

2) Evaluation of the optical Effectiveness of SWCNT layer

The operation of anti-reflective coatings is based on the physical principles of constructive and destructive interference of light waves, which arise from variations in the optical constants, such as the refractive indices of the layers [30]. When incident light strikes a multilayer surface with different refractive indices, a portion of the light is reflected at each interface between layers, while the remainder transmits into the next layer. The goal is to reduce the overall light reflection, which occurs over a specific wavelength range. In double-layer anti-reflective coatings, this process is achieved using two layers to broaden the effective wavelength range and enhance the reduction of reflection [31]. This design enhances light transmittance, making it particularly beneficial for applications in optics and photovoltaics [32].

Since PSCs have a multilayered structure, controlling light reflection at the interfaces between layers is of great importance. The incident light can be reflected at each interface between the layers before reaching the perovskite layer. Therefore, the selection of electron transport materials is crucial from an optical perspective, as the optical constants of these layers significantly affect the absorption and reflection of light [33].

The performed simulations present the light reflectance from the surface of the PSC before and after the incorporation of the carbon nanotube layer across various wavelengths, as shown in Fig. 7. The optical constants of the layers used in the proposed structure for simulation were extracted from references [34-37].

As can be seen in Fig. 7, the addition of the SWCNT layer reduces reflection in the visible wavelength range, particularly in the 0.4–0.8 µm region. This behavior can be explained by the principle of constructive and destructive interference in multilayer structures with different refractive indices. The presence of the SWCNT layer between the ITO and TiO₂ layers gradually changes the refractive index contrast, thereby reducing the sudden optical discontinuity and consequently lowering the reflection intensity from the cell surface. In fact, the SWCNT layer acts as an anti-reflection coating, enhancing light transmission into the perovskite absorber. The reduction in reflection within this spectral region is particularly significant because it overlaps well with the main absorption band of perovskite, and thus is expected to improve the photovoltaic conversion efficiency of the solar cell.

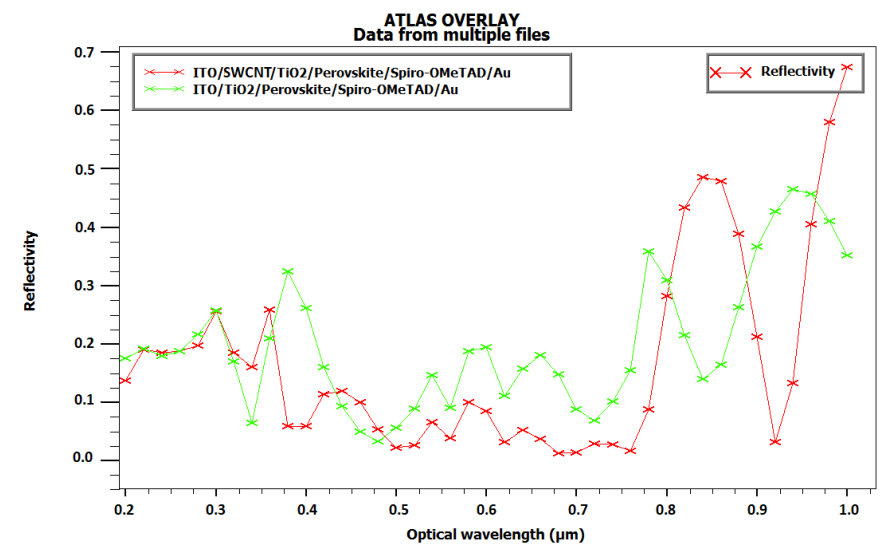


Fig. 7. Light reflection from the solar cell surface before and after incorporation of the SWCNT layer

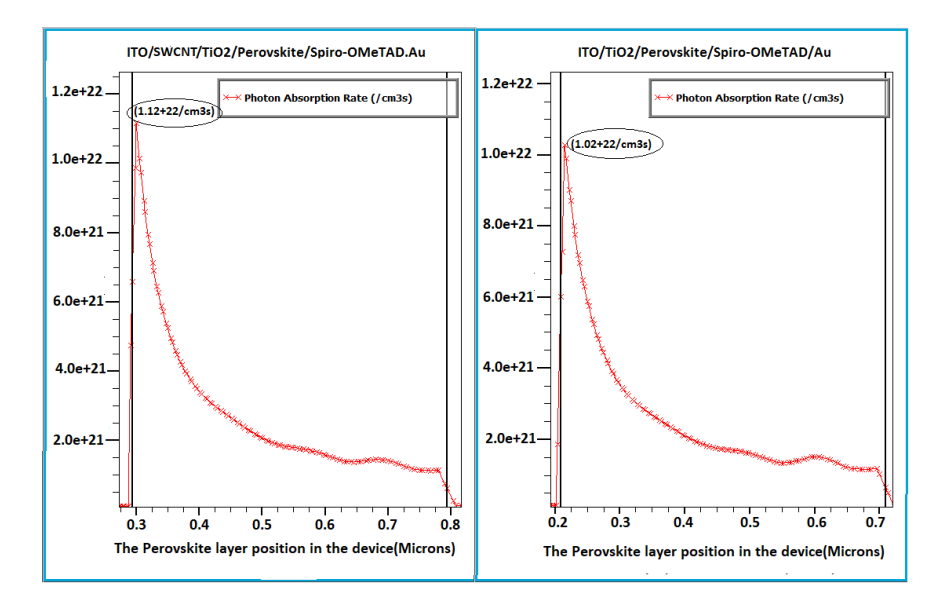


Fig. 8. Enhancement of photon absorption in the perovskite layer due to incorporation of the SWCNT layer

Furthermore, Fig. 8 shows the photon absorption in the perovskite layer after the incorporation of the SWCNT layer. The use of the SWCNT layer reduces the reflectance of light from the TiO₂ layer, allowing more light to be transmitted through this layer and absorbed by the perovskite layer.

The performance parameters of the proposed PSC compared to the simple structure-including open-circuit voltage (Voc), short-circuit current density (Jsc), fill factor (FF), and power conversion efficiency (PCE)—are presented in Table 3.

TABLE 3
Comparison of performance parameters of PSC with and without SWCNT layer

Solar Cell	$V_{oc}(v)$	J_{sc} (mA/cm ²)	FF	PCE
Simple PSC	1.12	20.39	84.97	19.4%
proposed PSC	1.12	21.41	84.92	20.39%

As observed from the simulation results in Table 3, incorporating the SWCNT layer into the PSC structure has resulted in an approximately 1% increase in PCE.

This increase in efficiency is due to the fact that, although more light is absorbed by the perovskite layer (the optical effect of the SWCNT layer), there is less recombination occurring in the perovskite layer (the electrical effect of the SWCNT layer), which ultimately leads to an increase in the short-circuit current density and PCE of the proposed solar cell.

3) Optimal Thickness of SWCNT Layer

Simulation results revealed that the incorporation of SWCNT layer into the PSC structure enhances device performance due to its electrical and optical contributions. Among the parameters influencing this effect, the SWCNT layer thickness plays a key role in determining performance parameters. Thickness variation alters the balance between electrical conductivity—affecting charge extraction efficiency—and optical transparency, which controls the intensity of light reaching the active perovskite layer. This section investigates the influence of SWCNT layer thickness on device efficiency to identify the optimal thickness for maximizing performance. The SWCNT layer thickness was varied between 80 and 130 nm. Fig. 9 illustrates the efficiency dependence on SWCNT thickness. The optimal thickness was determined to be 100 nm, yielding a maximum efficiency of 20.39%.

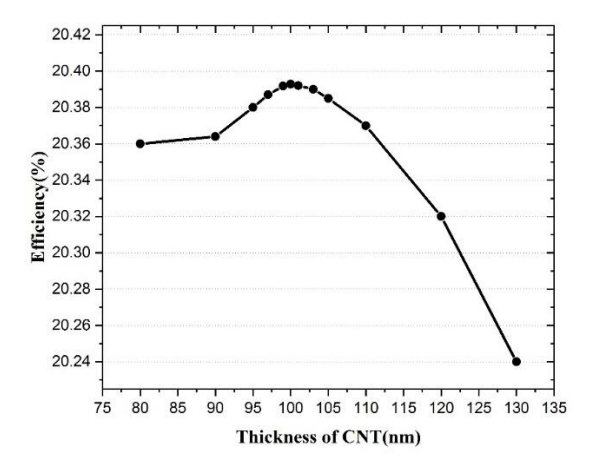


Fig. 9. Variation of efficiency as a function of SWCNT layer thickness

This optimal thickness arises from a trade-off between electrical conductivity and optical absorption effects. At thicknesses below 100 nm, insufficient conductivity reduces device efficiency due to limited charge transport. Conversely, at

thicknesses exceeding 100 nm, by increased optical absorption in the SWCNT layer, which decreases the light reaching the perovskite absorber and consequently lowers efficiency. This balance results in 100 nm being the most favorable thickness for achieving the highest device performance within the investigated range.

4) Evaluation of the Chirality Effect of SWCNT layer on the Performance of the Proposed Solar Cell

In this section, the effect of the chirality of the SWCNT incorporated in the structure on the solar cell efficiency is examined. As previously mentioned in Equations (7) and (8), chirality influences both the diameter and the bandgap of the nanotube. Additionally, optical studies indicate that changes in chirality alter the optical constants of the nanotube [34]. Consequently, the performance of the nanotube within the device structure is affected by the parameters related to its chirality. Table 4 presents the chirality, diameter of carbon nanotubes, their refractive index at a wavelength of 550 nm, and the corresponding solar cell efficiency.

TABLE 4
Effect of SWCNT chirality on the solar cell efficiency

Chirality	Diameter of SWCNT	Refractive index	PCE
(n,m)	(D_{cnt})	(n)	(%)
(6,5)	0.747	1.50	20.39
(8,3)	0.771	1.55	18.00
(9,2)	0.795	1.40	17.28
(9,4)	0.903	1.35	16.15
(10,3)	0.923	1.45	18.72

This table demonstrates that changes in the chirality indices of carbon nanotubes lead to variations in properties such as diameter and optical characteristics. Moreover, the data on refractive indices indicate that this parameter is not necessarily a monotonic function of diameter or chirality. Therefore, when nanotubes with different chiralities are incorporated into the solar cell structure, no straightforward correlation between efficiency and changes in nanotube diameter can be established. Hence, to increase the efficiency of the solar cell with the proposed structure, the chirality of the nanotube used becomes important.

5.CONCLUSION

This study investigated the performance of a SWCNT layer as a secondary ETL in a PSC. Simulation results demonstrated that incorporating this layer increases the conduction band slope within the perovskite absorber, thereby reducing the probability of charge carrier recombination in this layer. Since light must pass through the ETLs before reaching the perovskite layer, the optical effects of the SWCNT layer were also examined. The optical simulations revealed that the addition of the SWCNT layer reduces light reflection at the cell surface, leading to increased light absorption by the active layer. Furthermore, the effect of nanotube chirality was examined, and the optimal thickness of the SWCNT layer was determined. The results showed the highest efficiency at a thickness of 100nm and for carbon nanotubes with chirality (6,5). The power conversion efficiency of the proposed cell structure improved by approximately 1%.

References

- [1] E. Pulli, E. Rozzi, F. Bella, Transparent photovoltaic technologies: Current trends towards upscaling, Energy Conversion and Management 219 (2020) 112982.https://doi.org/10.1016/j.enconman.2020.112982
- [2] Z. Hu, C. Ran, H. Zhang, L. Chao, Y. Chen, W. Huang, The current status and development trend of perovskite solar cells, Engineering 21 (2023) 15-19.https://doi.org/10.1016/j.eng.2022.10.012
- [3] M. Roohollahi, M.R. Shayesteh, M. Pourahmadi, Improved perovskite solar cell performance using semitransparent CNT layer, (2023).https://jopn.marvdasht.iau.ir/article_5801.html
- [4] N.R.E. Laboratory. https://www.nrel.gov/pv/cell-efficiency
- [5] P. Zhao, Z. Lin, J. Wang, M. Yue, J. Su, J. Zhang, J. Chang, Y. Hao, Numerical simulation of planar heterojunction perovskite solar cells based on SnO2 electron transport layer, ACS Applied Energy Materials 2 (2019) 4504-4512. https://pubs.acs.org/doi/abs/10.1021/acsaem.9b00755
- [6] S. Rafiee Rafat, Z. Ahangari, M.M. Ahadian, Performance Investigation of a Perovskite Solar Cell with TiO2 and One Dimensional ZnO Nanorods as Electron Transport Layers, Journal of Optoelectronical Nanostructures 6 (2021) 75-90.https://jopn.marvdasht.iau.ir/article_4771.html
- [7] K.S. Kim, W. Lee, J.W. Jung, A cascade bilayer electron transport layer toward efficient and stable Ruddlesden-Popper perovskite solar cells, International Journal of Energy Research 46 (2022) 8229-8239. https://doi.org/10.1002/er.7725
- [8] C. Li, H. Xu, C. Zhi, Z. Wan, Z. Li, TiO2/SnO2 electron transport double layers with ultrathin SnO2 for efficient planar perovskite solar cells, Chinese Physics B 31 (2022) 118802.https://iopscience.iop.org/article/10.1088/1674-1056/ac8349/meta

- [9] Y. Zhou, X. Ren, S. He, Z. Huang, in: 2022 International Conference on Microwave and Millimeter Wave Technology (ICMMT), (IEEE, 2022). https://doi.org/10.1109/ICMMT55580.2022.10022712
- [10] W. Huang, R. Zhang, X. Xia, P. Steichen, N. Liu, J. Yang, L. Chu, X.a. Li, Room temperature processed double electron transport layers for efficient perovskite solar cells, Nanomaterials 11 (2021) 329. https://doi.org/10.3390/nano11020329
- [11] H.G. Lemos, J.H. Rossato, R.A. Ramos, J.V. Lima, L.J. Affonço, S. Trofimov, J.J. Michel, S.L. Fernandes, B. Naydenov, C.F. Graeff, Electron transport bilayer with cascade energy alignment based on Nb 2 O 5–Ti 3 C 2 MXene/TiO 2 for efficient perovskite solar cells, Journal of Materials Chemistry C 11 (2023) 3571-3580.https://doi.org/10.1039/D3TC00022B
- [12] T. Sewela, R. Ocaya, T. Malevu, Recent insights into the transformative role of Graphene-based/TiO2 electron transport layers for perovskite solar cells, Energy Science & Engineering 13 (2025) 4-26. https://doi.org/10.1002/ese3.1878
- [13] X. Sun, L. Li, S. Shen, F. Wang, TiO2/SnO2 bilayer electron transport layer for high efficiency perovskite solar cells, Nanomaterials 13 (2023) 249.https://doi.org/10.3390/nano13020249
- [14] D. Du, D. Zhang, H. Liu, W. Shen, Enhanced carrier transport and optical gains in perovskite solar cells based on low-temperature prepared TiO2@SnO2 nanocrystals, Journal of Alloys and Compounds 983 (2024) 173714.https://doi.org/10.1016/j.jallcom.2024.173714
- [15] A. Drygała, Z. Starowicz, K. Gawlińska-Nęcek, M. Karolus, M. Lipiński, P. Jarka, W. Matysiak, E. Tillová, P. Palček, T. Tański, Hybrid mesoporous TiO2/ZnO electron transport layer for efficient perovskite solar cell, Molecules 28 (2023) 5656.https://doi.org/10.3390/molecules28155656
- [16] M. Hadadian, J.-H. Smått, J.-P. Correa-Baena, The role of carbon-based materials in enhancing the stability of perovskite solar cells, Energy & Environmental Science 13 (2020) 1377-1407. https://doi.org/10.1039/C9EE04030G
- [17] S.N. jafari, A. Ghadimi, s. rouhi, Strained Carbon Nanotube (SCNT) Thin Layer Effect on GaAs Solar Cells Efficiency, Journal of Optoelectronical Nanostructures 5 (2020) 87-110.https://jopn.marvdasht.iau.ir/article_4505.html
- [18] J. Abraham, A. Reghunadhan, K. Nimitha, S.C. George, S. Thomas, in: Carbon Nanotubes, (Apple Academic Press, 2022). https://doi.org/10.1201/9781003277194
- [19] M. Roohollahi, M.R. Shayesteh, M. Pourahmadi, Simulation and efficiency improvement of perovskite solar cells using optimized carbon nanotube charge collector and molybdenum trioxide layer, Indian Journal of Physics 98 (2024) 4949-4959.https://doi.org/10.1007/s12648-024-03257-6
- [20] H.H. Madani, M.R. Shayesteh, M. Reza, A carbon nanotube (CNT)-based SiGe thin film solar cell structure, J Optoelectron Nanostruct Winter 6 (2021).http://dx.doi.org/10.30495/jopn.2021.4541
- [21] F. Arjmand, S.J. Fatemi, Improved performance of carbon-based perovskite solar cells using a multi-walled carbon nanotubes/Zn(COO)2 nanocomposite, Scientific Reports 15 (2025) 23488. https://www.nature.com/articles/s41598-025-08040-z

- [22] A.S.R. Bati, L. Yu, S.A. Tawfik, M.J.S. Spencer, P.E. Shaw, M. Batmunkh, J.G. Electrically Sorted Single-Walled Carbon Nanotubes-Based Electron Transporting Layers for Perovskite Solar Cells, iScience 14 (2019) 100-112.https://www.cell.com/iscience/fulltext/S2589-0042(19)30081-1
- [23] Y. Gan, G. Qiu, B. Qin, X. Bi, Y. Liu, G. Nie, W. Ning, R. Yang, Numerical analysis of stable (FAPbI3) 0.85 (MAPbBr3) 0.15-based perovskite solar cell with TiO2/ZnO double electron layer, Nanomaterials 13 (2023)1313.https://doi.org/10.3390/nano13081313
- [24] K. Pourchitsaz, M.R. Shayesteh, Self-heating effect modeling of a carbon nanotubebased fieldeffect transistor (CNTFET), Journal of Optoelectronical Nanostructures 4 (2019) 51-66.https://jopn.marvdasht.iau.ir/article 3385.html
- [25] B. Singh, B. Prasad, D. Kumar, DFT based estimation of CNT parameters and simulation-study of GAA CNTFET for nano scale applications, Materials Research 015916.https://iopscience.iop.org/article/10.1088/2053-(2020)1591/ab6924/meta
- [26] A. Hima, N. Lakhdar, B. Benhaoua, A. Saadoune, I. Kemerchou, F. Rogti, An optimized perovskite solar cell designs for high conversion efficiency, Superlattices and Microstructures 129 (2019) 240-246.https://doi.org/10.1016/j.spmi.2019.04.007
- [27] M.A. Islam, J. Al Rafi, M.A. Uddin, Modeling and formation of a single-walled carbon nanotube (SWCNT) based heterostructure for efficient solar energy: Performance defect analysis simulation. AIP Advances and by numerical (2023).https://doi.org/10.1063/5.0167228
- [28] N.E. Courtier, Modelling ion migration and charge carrier transport in planar cells (University Southampton, 2019). perovskite solar of HTTPS://EPRINTS.SOTON.AC.UK/433121/
- [29] M. Batmunkh, T.J. Macdonald, C.J. Shearer, M. Bat-Erdene, Y. Wang, M.J. Biggs, I.P. Parkin, T. Nann, J.G. Shapter, Carbon nanotubes in TiO2 nanofiber photoelectrodes high-performance perovskite solar cells, Advanced Science 4 (2017) 1600504.https://advanced.onlinelibrary.wiley.com/doi/full/10.1002/advs.201600504
- [30] H.A. Macleod, H.A. Macleod, Thin-film optical filters (CRC press, 2010).https://doi.org/10.1201/9781420073034
- [31] S. Chattopadhyay, Y.-F. Huang, Y.-J. Jen, A. Ganguly, K. Chen, L. Chen, Antireflecting and photonic nanostructures, Materials Science and Engineering: R: Reports 69 (2010) 1-35.https://doi.org/10.1016/j.mser.2010.04.001
- [32] F. Ahmad, B.J. Civiletti, P.B. Monk, A. Lakhtakia, in: International Workshop on Thin Films for Electronics, Electro-Optics, Energy and Sensors 2022, (SPIE, 2023).https://doi.org/10.1117/12.2645881
- [33] H. Zhang, X. Liang, Y. Zhang, Y. Chen, N.-G. Park, Unraveling Optical and Electrical Gains of Perovskite Solar Cells with an Antireflective and Energetic Cascade Electron Transport Layer, ACS Applied Materials & Interfaces 15 (2023) 21152-21161.https://pubs.acs.org/doi/abs/10.1021/acsami.3c02233
- [34] S. Elewa, B. Yousif, N.F. Areed, M.E.A. Abo-Elsoud, Harnessing SWCNT absorber based efficient CH3NH3PbI3 perovskite solar cells, Optical and Quantum Electronics 56 (2024) 1735.https://link.springer.com/article/10.1007/s11082-024-07419-y

[35] T.A. Konig, P.A. Ledin, J. Kerszulis, M.A. Mahmoud, M.A. El-Sayed, J.R. Reynolds, V.V. Tsukruk, Electrically tunable plasmonic behavior of nanocube–polymer nanomaterials induced by a redox-active electrochromic polymer, ACS nano 8 (2014) 6182-6192.https://pubs.acs.org/doi/abs/10.1021/nn501601e

[36] L.J. Phillips, A.M. Rashed, R.E. Treharne, J. Kay, P. Yates, I.Z. Mitrovic, A. Weerakkody, S. Hall, K. Durose, Dispersion relation data for methylammonium lead triiodide perovskite deposited on a (100) silicon wafer using a two-step vapour-phase reaction process, Data in brief 5 (2015) 926-928. https://doi.org/10.1016/j.dib.2015.10.026 [37] M. Filipič, P. Löper, B. Niesen, S. De Wolf, J. Krč, C. Ballif, M. Topič, CH 3 NH 3 PbI 3 perovskite/silicon tandem solar cells: characterization based optical simulations, Optics express 23 (2015) A263-A278. https://doi.org/10.1364/OE.23.00A263